ChemBioChem

Supporting Information

Broadening the Scope of the Flavin-Tag Method by Improving Flavin Incorporation and Incorporating Flavin Analogs

Yapei Tong, Marnix R. Loonstra, and Marco W. Fraaije*

Contents

Figure S1.

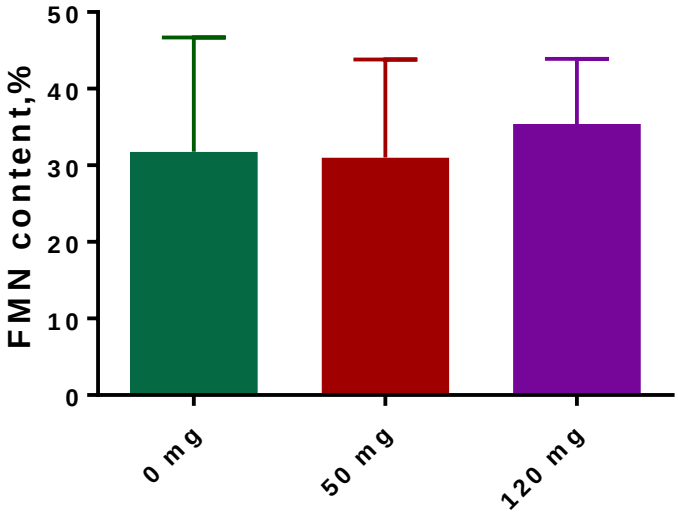

Figure S1. The effect of riboflavin content on FMN conjugation efficiency in *E. coli.* MBP-CF1 variant was used to evaluate the effect of riboflavin content on the modification efficiency. C = C-terminal tag, F1-tag = GVDGLSGATLTS.

Figure S2.

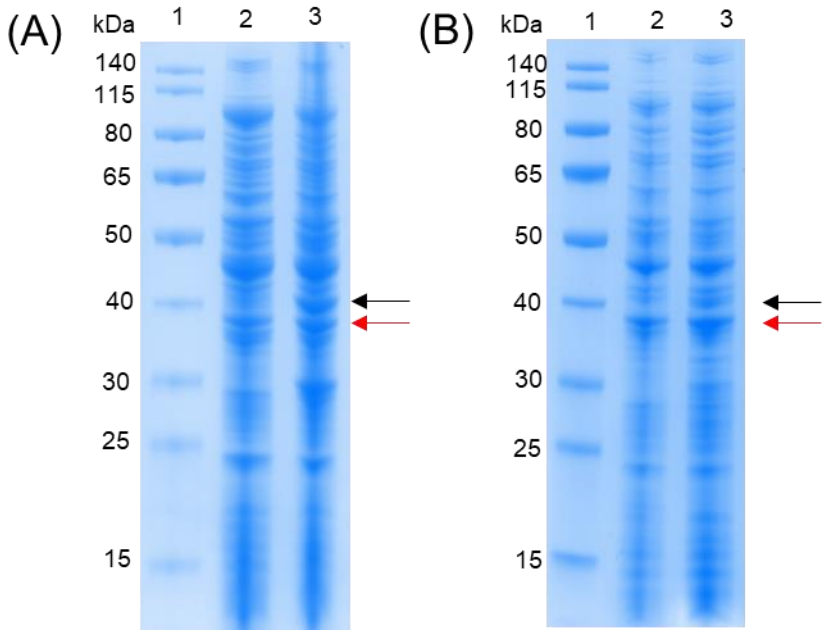

Figure S2. Polyacrylamide gel of whole cell extracts of *E. coli* BL 21-AI cells. pRSF-Duet-1 vector, carrying flavin transferase gene and FAD synthetase gene, was transformed into *E. coli* BL 21-AI cells. The whole cell extract was loaded on a polyacrylamide gel. (A) Cells were grown in 20 mL TB medium at 37 ºC overnight. (B) Cells were grown in 20 mL TB medium at 17 ºC for 24 h. Line 1 is protein marker, line 2 is BL 21-AI cell without plasmid, line 3 is BL21-AI cell carried pRSF-Duet-1 vector with AbpE and FADS. The arrows show the protein band of FADS (black) and ApbE (red).

Figure S3.

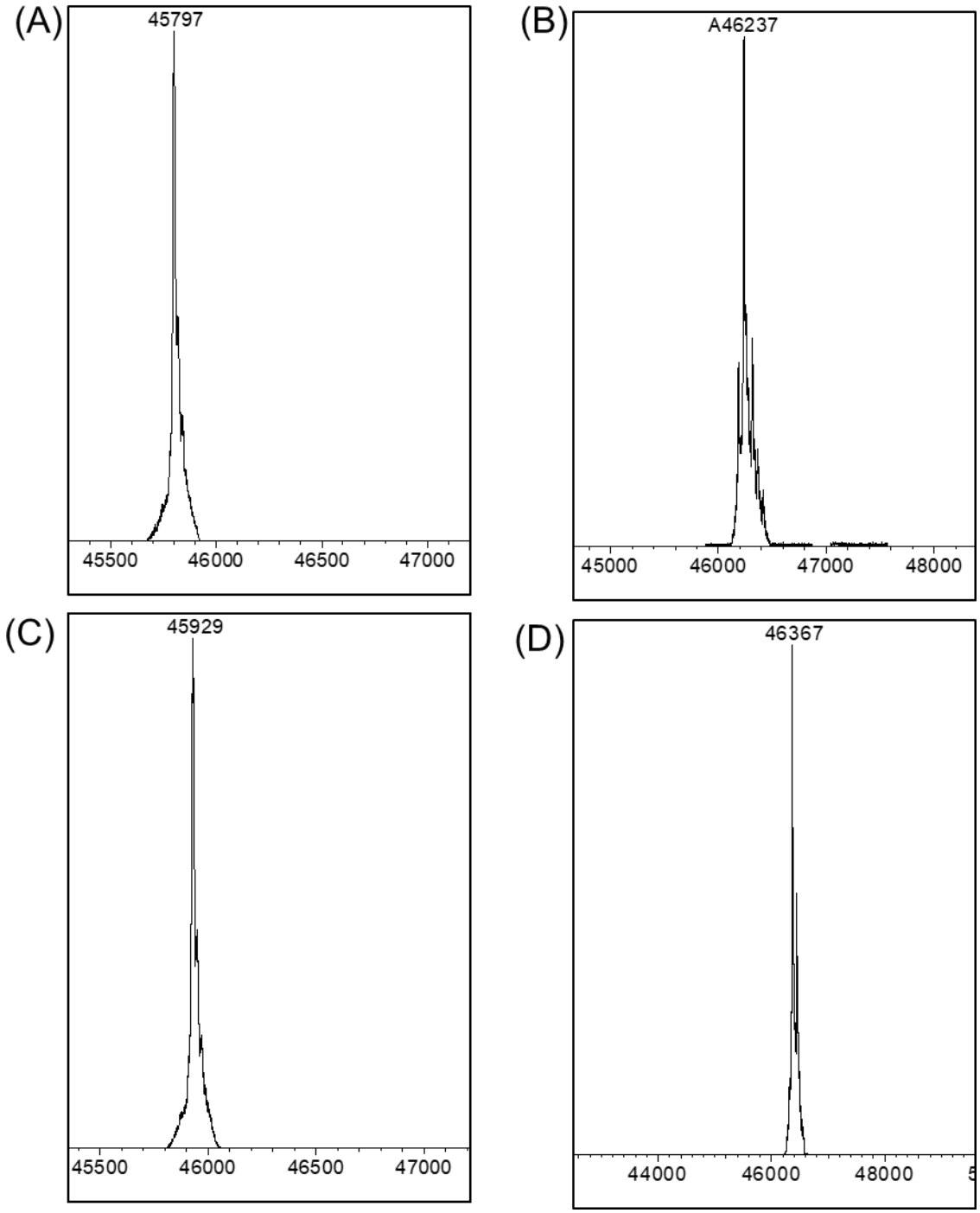

Figure S3. **Electrospray ionization mass analysis of MBP-NF1/CF1.** (A) MBP-NF1 was purified after expression in the absence of ApbE and FADS. The mass corresponds to the mass of unmodified MBP-NF1(45,797 Da) (B) MBP-NF1 was purified after coexpression in the presence of ApbE and FADS. The mass corresponds to the mass of FMN modified MBP-NF1(46,237 Da). (C) MBP-CF1 was purified after expression in the absence of ApbE and FADS. The mass corresponds to the mass of unmodified MBP-CF1(45,929 Da) (B) MBP-CF1 was purified after coexpression in the presence of ApbE and FADS. The mass corresponds to the mass of FMN modified MBP-CF1(46,367 Da). The cells were grown at 24 °C for 24 h. C=C-terminal tag, F1-tag=GVDGLSGATLTS.

Figure S4.

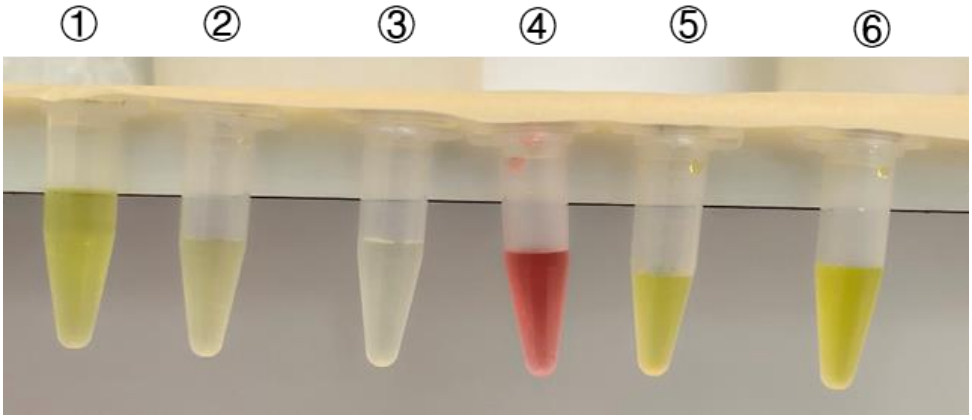

Figure S4. FAD derivatives. ① FAD, ② 7,8-dichloro-FAD, ③ 5-deaza-FAD, ④ roseo-FAD, ⑤ 7-methyl-8-ethyl-FAD, ⑥ 7-ethyl-8-methyl-FAD.

Figure S5.

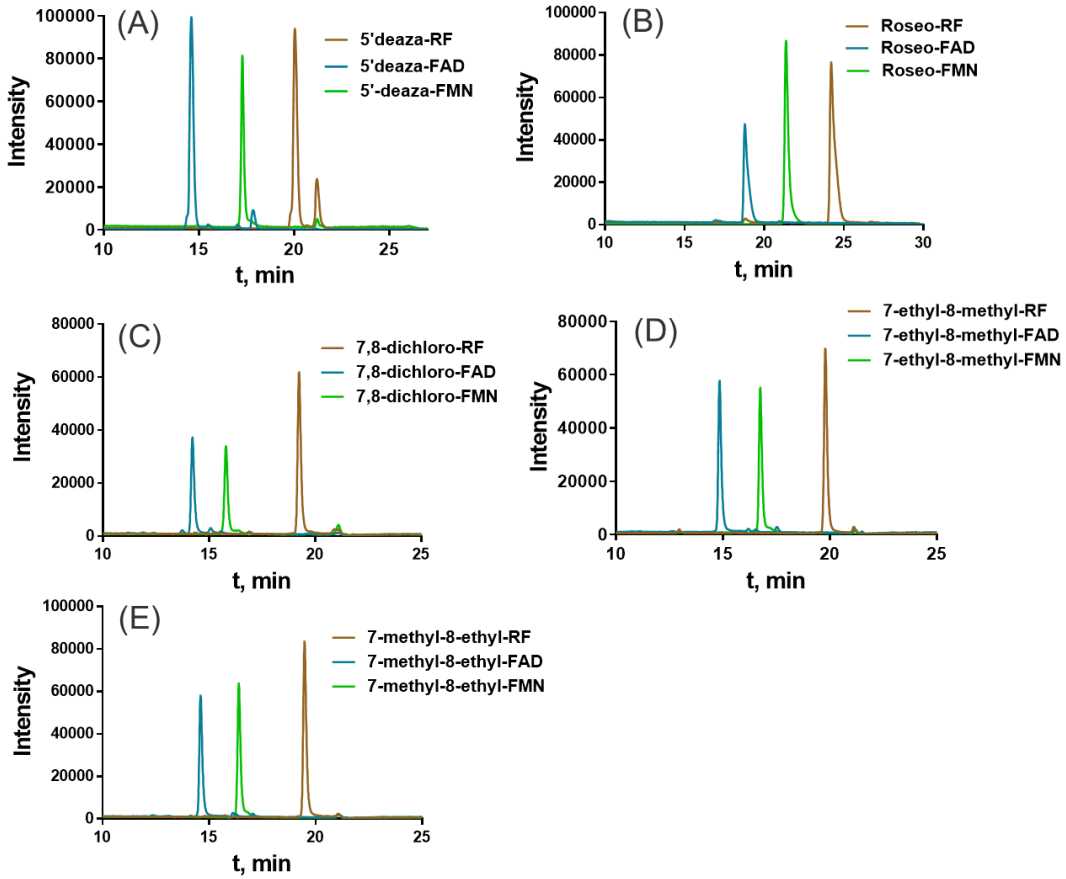

Figure S5. **HPLC chromatograms of riboflavin analogs and related FAD derivatives.** HPLC chromatograms of: (A) 5-deaza-RF (20.03 min), 5-deaza-FMN (17.02 min) and 5-deaza-FAD (14.6 min). (B) Roseo-RF (24 min), roseo-FMN (21.37 min) and roseo-FAD (19 min). (C) 7,8-dichloro-RF (19.2 min), 7,8-dichloro-FMN (15.79 min) and 7,8-dichloro-FAD (14.2 min). (D) 7-ethyl-8-methyl-RF (19.8 min), 7-ethyl-8-methyl-FMN (16.74 min) and 7-ethyl-8-methyl-FAD (14.8 min), (E) 7-methyl-8-ethyl-RF (19.5 min), 7-methyl-8-ethyl-FMN (16.40min) and 7-methyl-8-ethyl-FAD (14.6 min). The standard enzymatic reactions were carried out with 15 µM of purified recombinant FADS for FAD derivatives synthesis or 12 µM of purified CaRFK for FMN derivatives synthesis. The reactions were incubated for 16 h at 25˚C and analyzed with HPLC. The flavins, FMN derivatives, and FAD derivatives were purified by chromatography using a C18 column as described in Materials and Methods.

Figure S6.

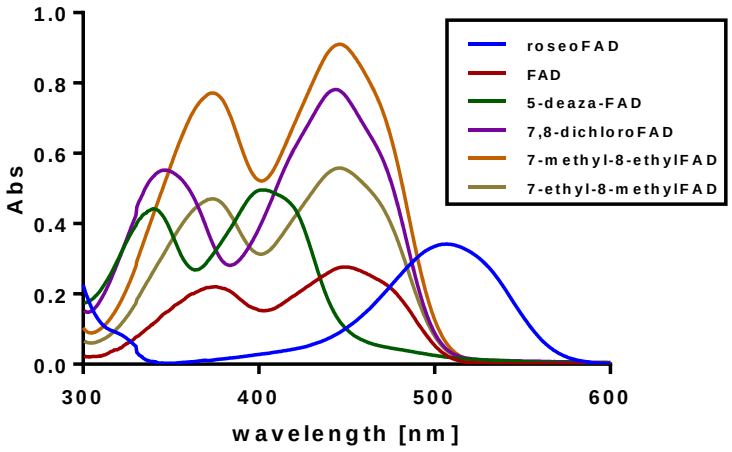

Figure S6. **UV-visible absorption spectra of FAD derivatives.**

Figure S7.

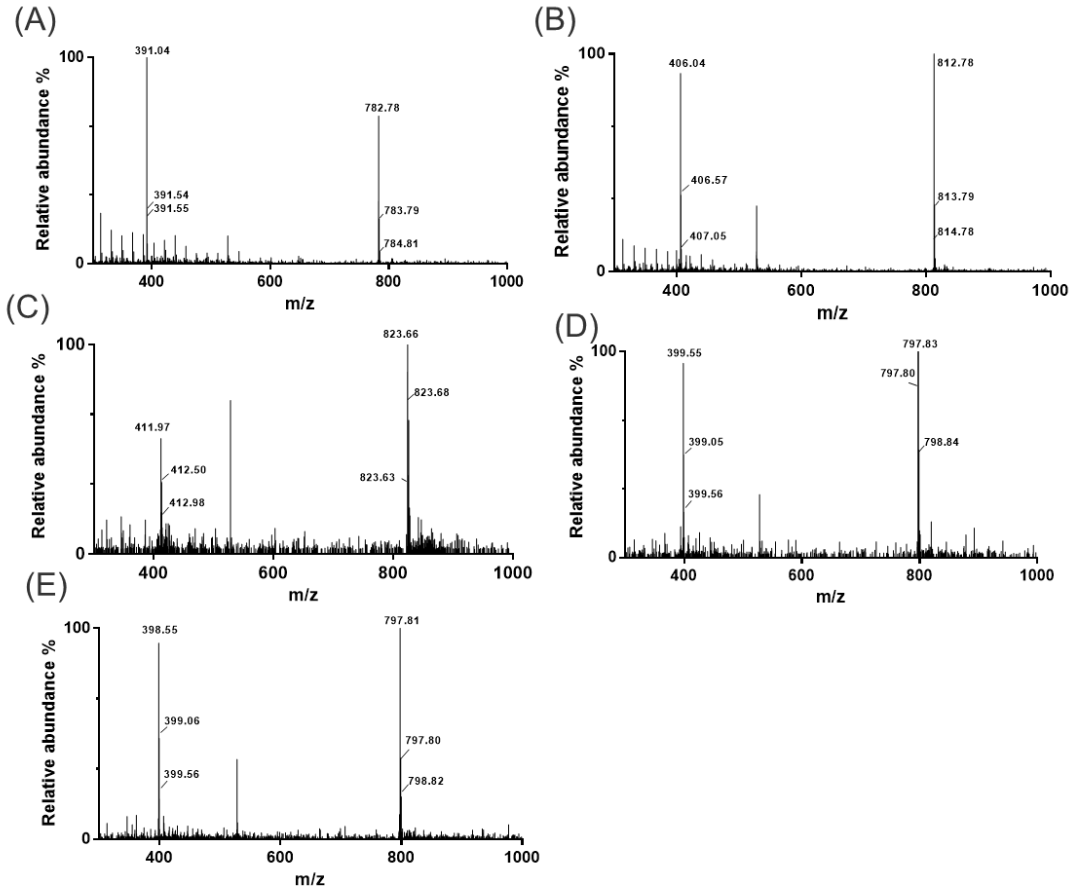

Figure S7. **LC-ESI-MS spectra (negative ion mode) of FAD derivatives enzymatically catalyzed by FADS**. Mass spectra of (A) 5-deazaFAD, m/z calculated: 783.14 $[M-H]^-$, 391.07 $[M-2H]^{2-}$; m/z observed: 782.78 $[M-H]^-$, 391.04 $[M-2H]^{2-}$. (B) roseo-FAD, m/z calculated: 813.17 $[M-H]^-$, 406.08 $[M-H]^{2-}$; m/z observed: 812.78$[M-H]^-$, 406.04 $[M-2H]^{2-}$.(C) 7,8-DichloroFAD, m/z calculated: 824.03 $[M-H]^-$, 411.51 $[M-2H]^{2-}$; m/z observed: 823.66$[M-H]^-$, 411.97 $[M-2H]^{2-}$. (D) 7-methyl-8-methyl-FAD, m/z calculated: 798.16 $[M-H]^-$, 398.58 $[M-2H]^{2-}$; m/z observed: 797.83$[M-H]^-$, 399.56 $[M-2H]^{2-}$. (E) 7-ethyl-8-methyl-FAD, m/z calculated: 798.16 $[M-H]^-$, 398.58 $[M-2H]^{2-}$; m/z observed: 797.81$[M-H]^-$, 398.55 $[M-2H]^{2-}$.

Figure S8.

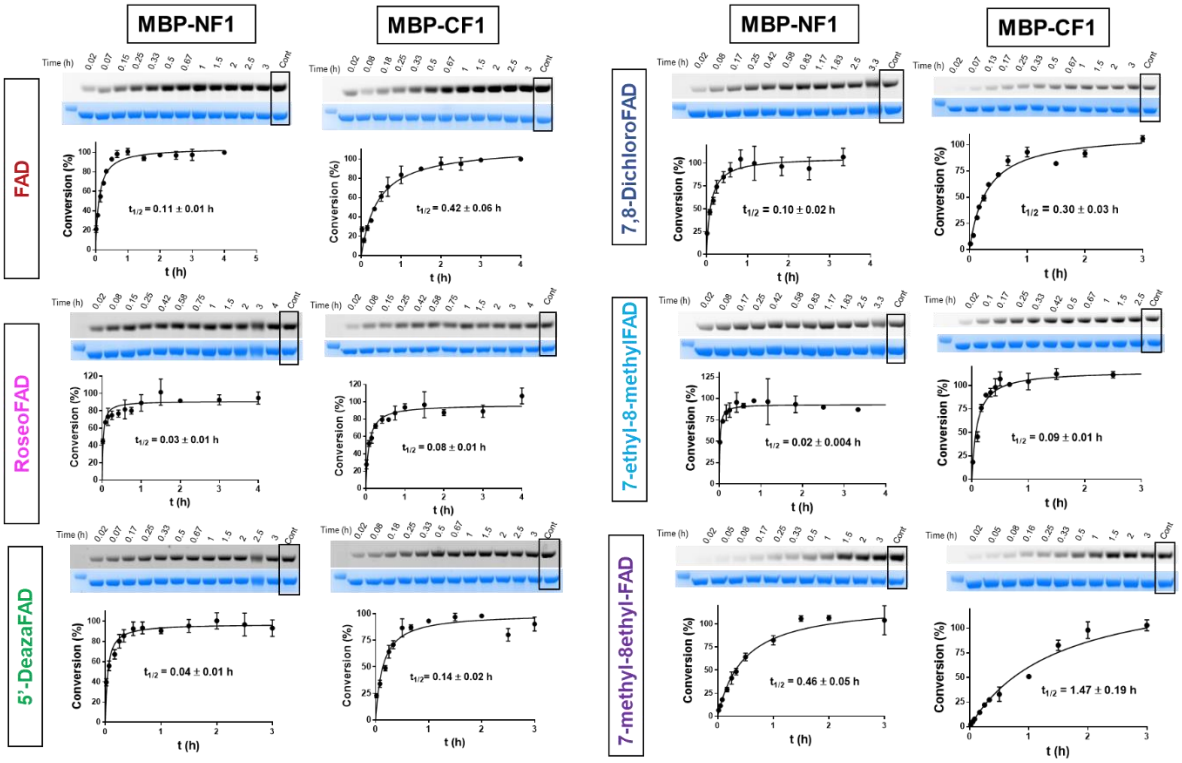

Figure S8. **Time-dependent analysis of flavinlytation of F1 tagged MBP by in-gel fluorescence.** All the reactions were performed in 50 mM Tris-HCl buffer, pH 8. The reactions contained 60 µM MBP, 10 mM Mg^{2+}, 20 µM ApbE and 1 mM FAD derivatives. Time-dependent samples were analyzed on In-gel fluorescence, which were evaluated by densitometry using ImageJ. The resulting densities were converted into percentages using the control band, which contained fully modified protein, and plotted against the time.

Figure S9.

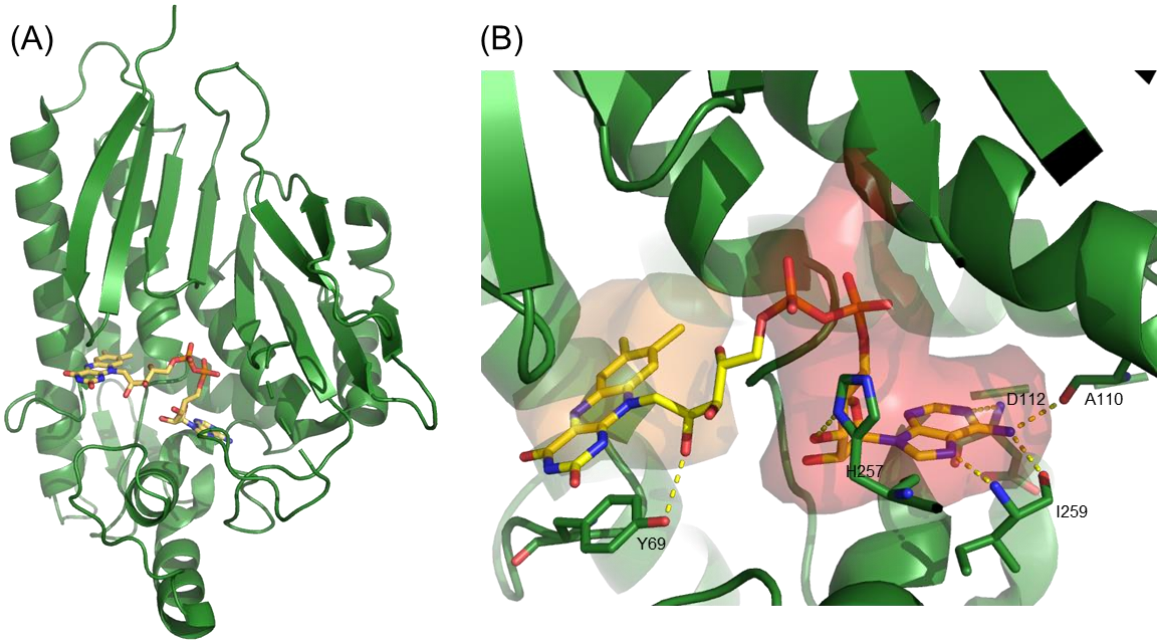

Figure S9. Crystal structure of VcApbE and its FAD binding pocket. (A) *V. cholerae* ApbE overall structure. FAD is shown in sticks. (B) A close-up view of the FAD binding pocket of VcApbE.

Figure S10.

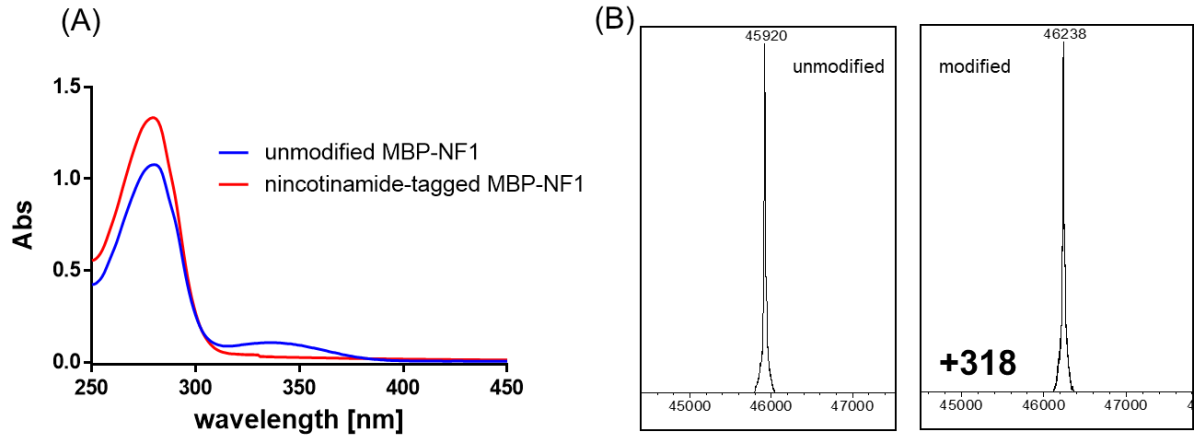

Figure S10. Absorbance spectrum and mass spectral analysis of nicotinamide-tagged MBP-NF1. (A) absorbance spectrum of unmodified MBP-NF1(red) and nicotinamide-tagged MBP-NF1(blue). (B) Electrospray ionization mass spectral analysis of unmodified MBP-NF1 (45,920 Da) and nicotinamide labeled MBP-NF1 (46,238 Da). The mass difference (318 Da) corresponds to the mass of nicotinamide part from NADH. The reaction was carried out in the Tris-HCl buffer at pH 8, containing 60 μM MBP-NF1, 10 mM Mg^{2+}, 30 mM NADH and 20 μM ApbE for 24 hours. Then the labeled protein was purified by using Ni^{2+} affinity chromatography from the reaction mixture, 100% modified MBP-NF1 was observed by ESI-MS.

Figure S11.

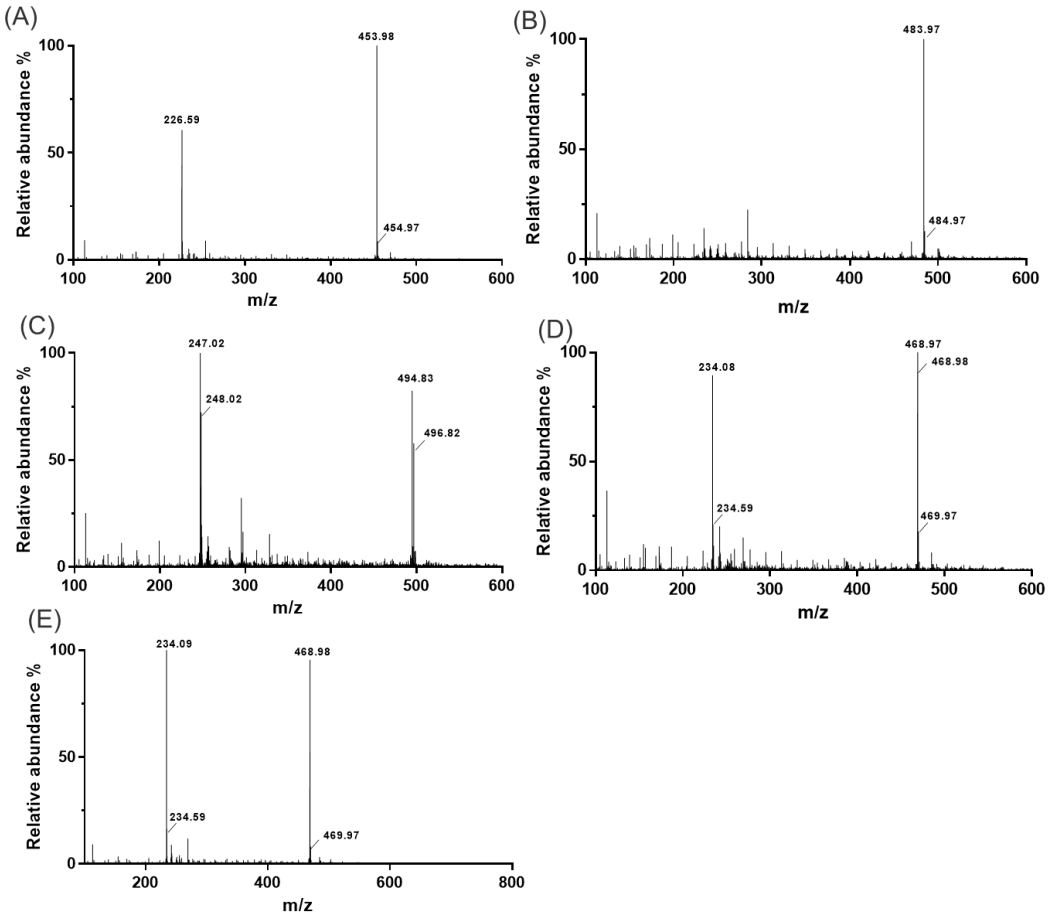

Figure S11. **LC-ESI-MS spectra (negative ion mode) of FMN derivatives enzymatically catalyzed by CaRFK.** Mass spectra of (A) 5-deazaFMN, m/z calculated: 453.10 $[M-H]^-$, 226.05 $[M-2H]^{2-}$; m/z observed: 453.98 $[M-H]^-$, 226.59 $[M-2H]^{2-}$. (B) roseoFMN, m/z calculated: 484.13 $[M-H]^-$; m/z observed: 483.97 $[M-H]^-$. (C) 7,8-DichloroFMN, m/z calculated: 495.00 $[M-H]^-$, 247.00 $[M-2H]^{2-}$; m/z observed: 494.83 $[M-H]^-$, 247.02 $[M-2H]^{2-}$. (D) 7-methyl-8-methyl-FMN, m/z calculated: 469.12 $[M-H]^-$, 234.06 $[M-2H]^{2-}$; m/z observed: 468.97 $[M-H]^-$, 234.08 $[M-2H]^{2-}$. (E) 7-ethyl-8-methyl-FMN, m/z calculated: 469.12 $[M-H]^-$, 234.06 $[M-2H]^{2-}$; m/z observed: 468.98 $[M-H]^-$, 234.09 $[M-2H]^{2-}$. The reactions were carried out by incubating 100 μM riboflavin analogs with 10 μM CaRFK in a volume of 50 mL at 25 °C for 16 h. The products were purified from the reaction mixture with the aid of a Reveleris C18-WP Flash cartridge column and were concentrated by freeze-drying.

Figure S12

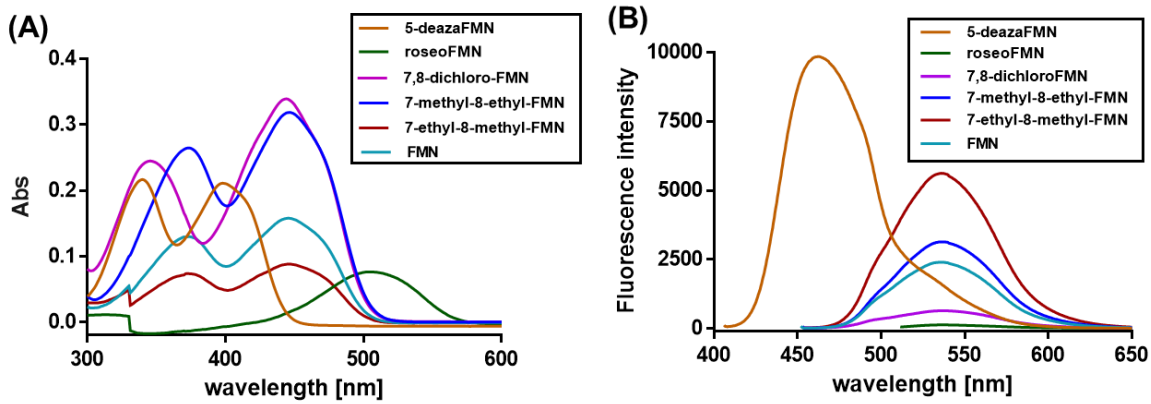

Figure S12. Absorption and emission spectra of the FMN derivatives. (A) The absorption spectrum of FMN derivatives synthesized by CaRFK. (B). Emission spectra of FMN derivatives were obtained by exciting the samples at an excitation wavelength, which was based on the maximum absorption of FMN derivatives and measuring the fluorescence emission in a range of 410−700 nm.

Figure S13.

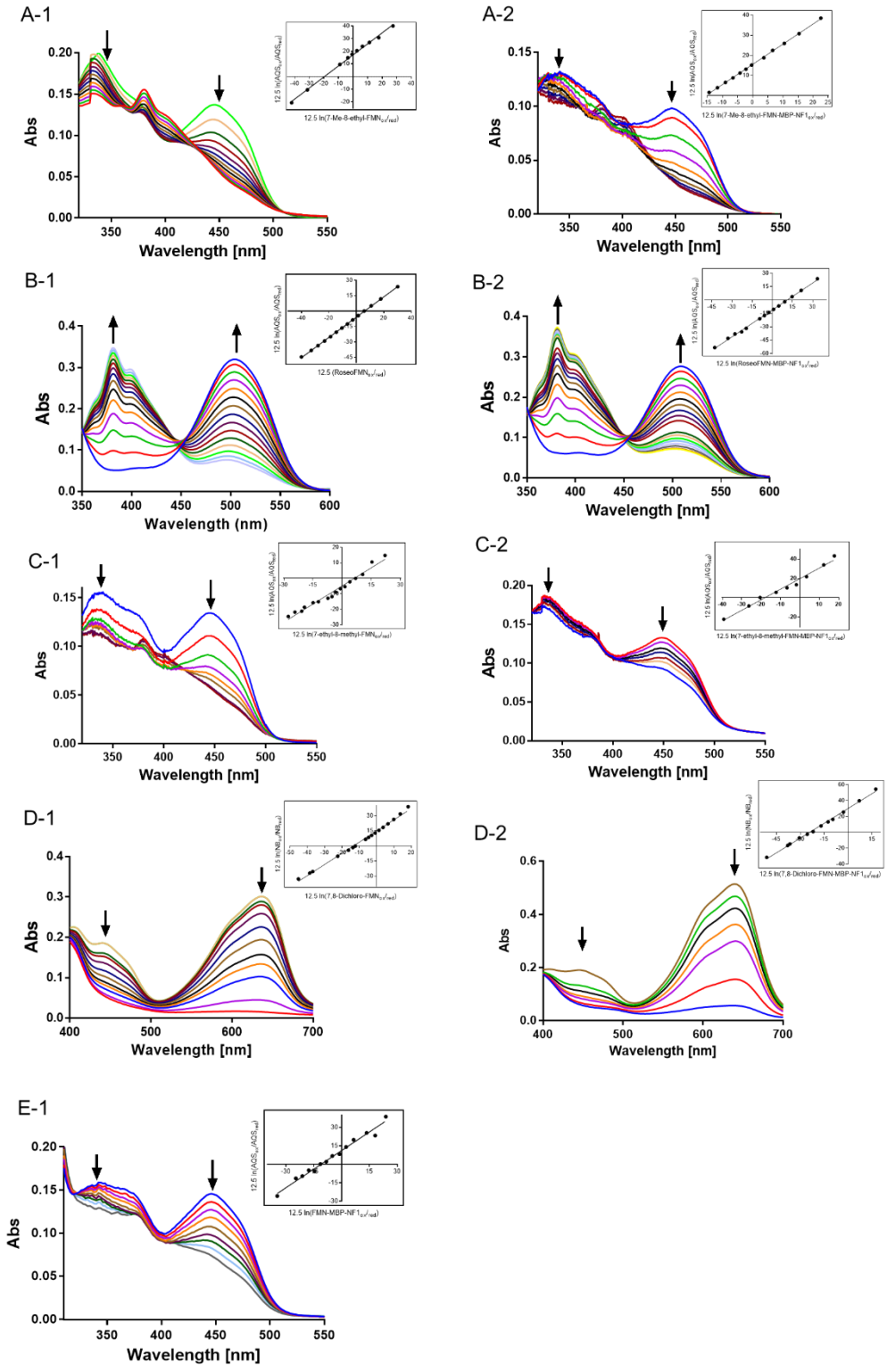

Figure S13. Determination of the midpoint potential (E_m) of FMN derivatives and FMN derivatives modified MBP variants using xanthine/xanthine oxidase system. (A) The redox potential measurement of 7-methyl-8-ethyl-FMN (A-1) and 7-methyl-8-ethyl-FMN modified MBP (A-2). (B) The redox potential measurement of roseo-FMN (B-1) and roseo-FMN modified MBP (B-2). (C) The redox potential measurement of 7-ethyl-8-methyl-FMN(C-1) and

7-ethyl-8-methyl-FMN modified MBP (C-2). (D) The redox potential measurement of 7,8-dichloro-FMN (D-1) and 7,8-dichloro-FMN modified MBP (D-2). (E) The redox potential measurement of FMN modified MBP. Selected spectra were obtained during the anaerobic reduction of FMN derivatives or FMN derivatives modified MBP (10-15 μM) in 50 mM Kpi (pH 7.0), containing 400 μM xanthine, 5 μM benzyl viologen, 50 mM glucose, 5 μg/ml catalase, 50 μg/ml glucose oxidase. Spectra were recorded at different time after the addition of catalytic amount of xanthine oxidase. The inset shows the Nernst plot (two independent measurements). The redox potential of FMN derivatives/ FMN derivatives modified MBP are shown in **Table 2**.

Figure S14.

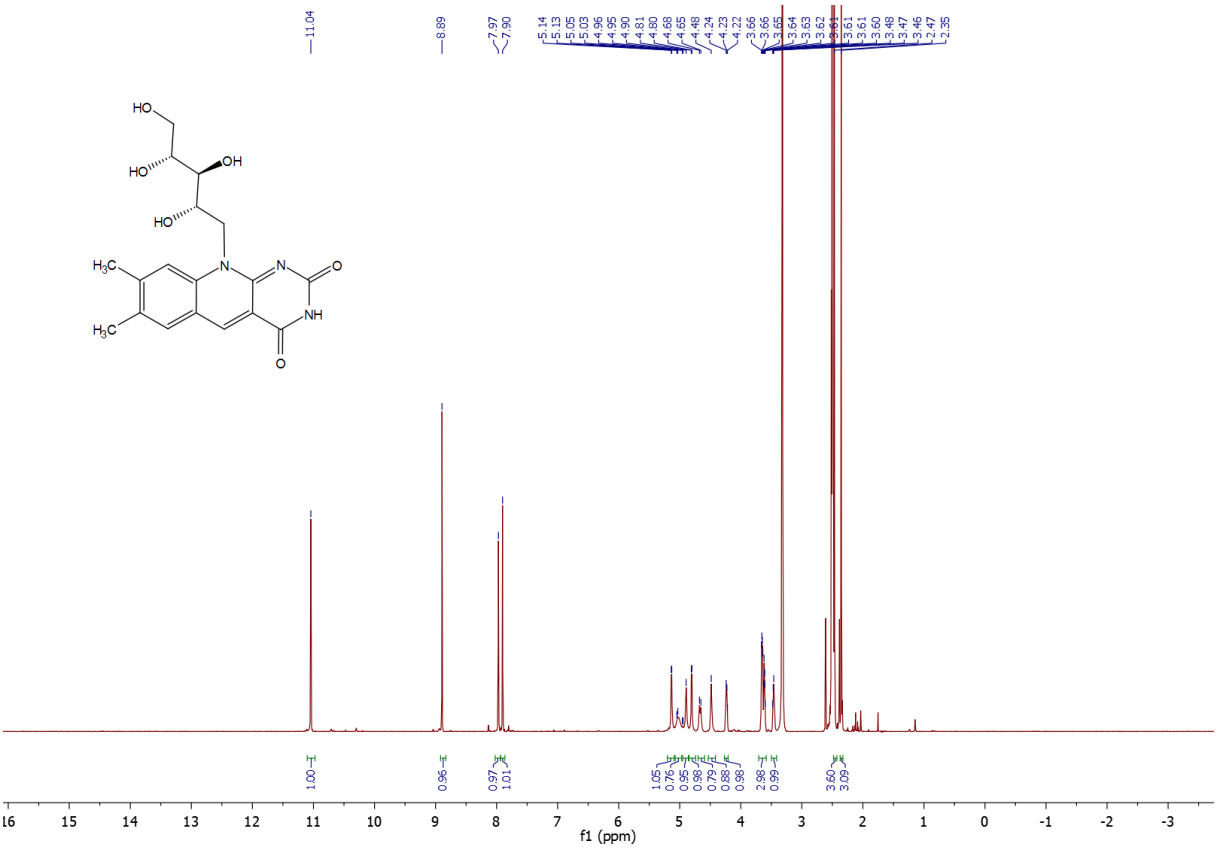

Figure S14. ^{1}H NMR spectra of 5-deazariboflavin.

Table S1. Protein sequences

Protein	Amino acid sequence
ApbE	MEKPAEQVHLSGPTMGTTYNIKYIQQPGIADSKILQTEIDRLL EEVNDQMSTYRKDSELSRFNQHTSSEPFAVSTQTLTVVKEAI RLNGLTEGALDVTVGPLVNLWGFGPEARPDVVPTDEELNAR RAITGIEHLTIEGNTLSKDIPELYVDLSTIAKGWGVDVVADYL QSQGIENYMVEIGGEIRLKGLNRDGVPWRIAIEKPSVDQRSV QEIIEPGDYAIATSGDYRNYFEQDGVRYSHIIDPTTGRPINNRV VSVTVLDKSCMTADGLATGLMVMGEERGMAVAEANQIPVL MIVKTDDGFKEYASSSFKPFLSK
MBP-N-F1	MGVDGLSGATLTSGGMKIEEGKLVIWINGDKGYNGLAEVG KKFEKDTGIKVTVEHPDKLEEKFPQVAATGDGPDIIFWAHDR FGGYAQSGLLAEITPDKAFQDKLYPFTWDAVRYNGKLIAYPI AVEALSLIYNKDLLPNPPKTWEEIPALDKELKAKGKSALMFN LQEPYFTWPLIAADGGYAFKYENGKYDIKDVGVDNAGAKA GLTFLVDLIKNKHMNADTDYSIAEAAFNKGETAMTINGPWA WSNIDTSKVNYGVTVLPTFKGQPSKPFVGVLSAGINAASPNK ELAKEFLENYLLTDEGLEAVNKDKPLGAVALKSYEEELAKD PRIAATMENAQKGEIMPNIPQMSAFWYAVRTAVINAASGRQ TVDEALKDAQTNSSSNNNNNNNNNNLGIEGRI
MBP-C-F1	MKIEEGKLVIWINGDKGYNGLAEVGKKFEKDTGIKVTVEHP DKLEEKFPQVAATGDGPDIIFWAHDRFGGYAQSGLLAEITPD KAFQDKLYPFTWDAVRYNGKLIAYPIAVEALSLIYNKDLLPN PPKTWEEIPALDKELKAKGKSALMFNLQEPYFTWPLIAADGG YAFKYENGKYDIKDVGVDNAGAKAGLTFLVDLIKNKHMNA DTDYSIAEAAFNKGETAMTINGPWAWSNIDTSKVNYGVTVL PTFKGQPSKPFVGVLSAGINAASPNKELAKEFLENYLLTDEG LEAVNKDKPLGAVALKSYEEELAKDPRIAATMENAQKGEIM PNIPQMSAFWYAVRTAVINAASGRQTVDEALKDAQTNSSSN NNNNNNNNLGIEGRIGGGVDGLSGATLTS
FADS	MDIWYGTAAVPKDLDNSAVTIGVFDGVHRGHQKLINATVEK AREVGAKAIMVTFDPHPVSVFLPRRAPLGITTLAERFALAESF GIDGVLVIDFTRELSGTSPEKYVEFLLEDTLHASHVVVGANFT FGENAAGTADSLRQICQSRLTVDVIDLLDDEGVRISSTTVREF LSEGDVARANWALGRHFYVTGPVVRGAGRGGKELGFPTAN QYFHDTVALPADGVYAGWLTILPTEAPVSGNMEPEVAYAAA ISVGTNPTFGDEQRSVESFVLDRDADLYGHDVKVEFVDHVR AMEKFDSVEQLLEVMAKDVQKTRTLLAQDVQAHKMAPETY FLQAES
CaRFK	MFYVTGPVVRGAGRGGKELGFPTANQYFHDTVALPADGVY AGWLTILPTEAPVSGNMEPEVAYAAAISVGTNPTFGDEQRSV ESFVLDRDADLYGHDVKVEFVDHVRAMEKFDSVEQLLEVM AKDVQKTRTLLAQDVQAHKMAPETYFLQAES

Flavin-tag (F1 tag) sequence is shown in red.

Table S2. All the constructs that are used in this work

Vectors	**proteins**
pBAD-NHis6x-SUMO/pBAD-no-tag	AbpE
pRSF-Duet-1	FADS/ApbE
pBAD-NHis6x	FADS/CaRFK/MBP/SUMO/ADH

SUMO: Small Ubiquitin-like Modifier

Table S3. All the primers that are used in this work

	Forward primer (5'-3')	Reverse primers (5'-3')
FADS	GGGAATTCCATATGGA TATTTGGTACGGA	GCCTTAATTAATTAGC TTTCTGCTTGTAG
ApbE	ATACATGCCATGGAG AAGCCGGCGGAG	GCCCAAGCTTTTACTT CGATAAAAAAGGC

Table S4. Biochemical/biophysical parameters for FMN derivatives

Compound	λ max (nm)	ε (M^{-1} cm^{-1})	Emission range (nm)
FMN	446	12,200	460-650
5-deaza-FMN	400	11,500	410-600
Roseo-FMN	505	22,200	520-650
7,8-dichloro-FMN	444	11,700	460-650
7-methyl-8-ethyl-FMN	447	11,700	460-650
7-ethyl-8-methyl-FMN	447	11,700	460-650